Pulse time modulation techniques for optical communications: a review

B. Wilson
Z. Ghassemlooy

Indexing terms: Modulation, Optical fibres, Telecommunications

Abstract: The principal factor in realising a high-performance bandwidth-efficient fibre communication system at an acceptable cost is the choice of modulation format on the optical carrier. In this context, pulse time modulation (PTM) techniques represent an attractive alternative to purely digital or analogue methods. The PTM family is reviewed, a classification system is proposed and their potential for use in high-speed fibre systems intended for the transmission of analogue data is examined.

1 Introduction

Optical fibre networks are being used to provide broadband telecommunication services that utilise multiplexes of video, data and voice channels. The choice of modulation format on the optical carrier is therefore a principal factor in realising a high-performance bandwidth-efficient system at an acceptable cost. Even though the bandwidths offered by new fibre installations are very high, they are still limited by fibre dispersion and carrier incoherence over practical distances.

Analogue modulation schemes, in which the optical source is modulated in a continuous manner, are both simple and bandwidth-efficient, but often cannot deliver the required signal-to-noise ratio. In addition, these schemes suffer to a certain extent from nonlinearity of the optical channel and associated circuitry, severely limiting the quality of the received information through intermodulation and crosstalk. In contrast, digital schemes such as pulse code modulation (PCM) have been demonstrated to be substantially immune to channel nonlinearity, and are capable of producing the required signal-to-noise ratio. However, digital systems are significantly more complex and costly than analogue systems, largely due to their coding circuitry and intrinsically large bandwidth overhead. This overhead can be reduced to that of analogue schemes by employing code compression, but complexity then increases significantly and so the overall cost remains high.

Pulse time modulation (PTM) represents an alternative approach that occupies an intermediate position between analogue and digital forms. Modulation is simple, requiring no digital coding, and the pulse format of the modulated carrier renders the scheme immune to channel nonlinearity and allows routing through logic circuits and switching nodes in a network. Moreover, PTM is unique in its ability to trade performance with bandwidth overhead, which is a particularly exploitable feature in fibre systems. For example, certain short-distance applications, such as local area networks (LANs), may use multimode or monomode fibre with a dispersive optical carrier, which imposes a significant bandwidth limitation in the optical channel. In these applications low-speed optical sources such as light emitting diodes (LEDs) can be used, while still achieving the required signal-to-noise ratio. In contrast, the available bandwidth on long-distance terrestrial and undersea routes may be many orders of magnitude broader where optical amplification and soliton techniques are employed. This additional bandwidth can be readily exploited by PTM to improve performance and signal-to-noise ratio. The ability to exchange signal-to-noise performance against bandwidth extension is a property unique to PTM modulation techniques, and is of increasing importance in high-speed networks. PTM techniques are of particular interest where short pulses, such as solitons, may be employed, since further forms of coding can yield further significant improvements over PCM.

The adoption of PTM techniques has certain beneficial consequences from the standpoint of optoelectronic subsystem specifications. As PTM deals exclusively with a pulse format, there are no concerns over LED or laser diode linearity, as would be the case with direct intensity modulation or subcarrier multiplexing techniques. In addition, for narrow-pulse PTM formats the peak optical output may be maintained at a high level to ensure good noise performance at the receiver without compromising device lifetime through elevated mean transmitter power levels. An optical transmitter for a PTM system may therefore be chosen primarily for its maximum peak power level; to maximise transmission distance and signal-to-noise performance with little regard for device

Paper 9753J (E13), first received 1st February and in revised form 21st June 1993

B. Wilson heads the Fibre Communications Research Group, Department of Electrical Engineering & Electronics, University of Manchester Institute of Science and Technology, PO Box 88, Manchester M60 1QD, United Kingdom

Z. Ghassemlooy is with the Communications Group, School of Engineering IT, Sheffield Hallam University, Pond Street, Sheffield S1 1WB, United Kingdom

The authors extend their gratitude to a number of research students who have over the last 8 years contributed to various aspects of the rolling programme of research into pulse time modulation techniques as UMIST, some of whom have been wholly or partially funded by the UK Science and Engineering Research Council.

linarity. LEDs are attractive in both cost-effectiveness and circuit simplicity, but inevitably suffer from restricted transmission distance through fibre dispersion limitations at shorter wavelengths, whereas injection laser diodes offer higher launch powers for longer wavelength systems.

2 Pulse time modulation family

The basic framework of research into PTM techniques was laid down around 50 years ago and reported in the late 1940s [1–4], but it is only recently that a revival of interest has been experienced, with the development of fibre transmission systems.

In all PTM methods, one of a range of time-dependent features of a pulsed carrier is used to convey information in preference to the carrier amplitude, as illustrated in Fig. 1. In pulsewidth modulation (PWM), sometimes

PTM type	Variable
PPM	Position
PWM	Width (duration)
PIM	Interval (space)
PIWM	Interval and width
PFM	Frequency
SWFM	Frequency

Fig. 1 *The PTM family*

referred to as pulse duration modulation (PDM), the width of the pulsed carrier within a predetermined timeframe is changed according to the sampled value of the modulating signal (Fig. 2*a*). Pulse position modulation (PPM) may be considered as differentiated PWM, and carries information by virtue of the continuously variable position of a narrow pulse within a fixed timeframe, as in Fig. 2*b*. Digital PPM employs discrete time slots to represent expanded PCM (Fig. 2*c*).

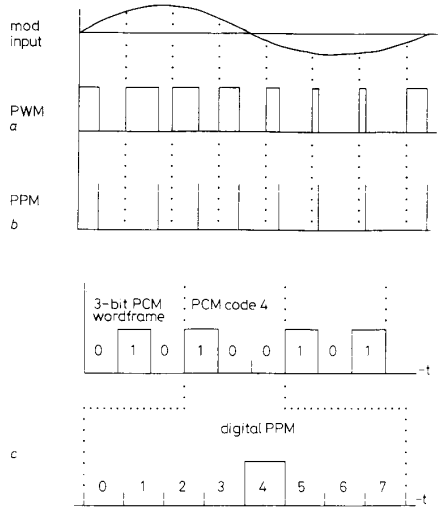

Fig. 2 *Isochronous PTM techniques*
a PWM
b PPM
c Digital PPM

As its name suggests, in pulse interval modulation (PIM) the variable intervals between adjacent narrow pulses are determined by the amplitude of the input signal (Fig. 3*a*). Pulse interval and width modulation (PIWM) is derived directly from PIM to produce a waveform in which both mark and space convey information in alternating sequence (Fig. 3*b*). Each successive timeframe in both PIM and PIWM commences immediately after the previous pulse, unlike PWM and PPM, which have fixed timeframes allocated for sampling.

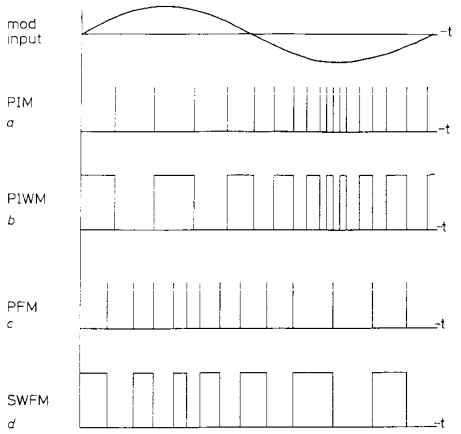

Fig. 3 *Anisochronous PTM*
a PIM
b PIWM
c PFM
d SWFM

In pulse frequency modulation (PFM), the instantaneous frequency of a train of narrow pulses is determined by the modulating signal amplitude (Fig. 3*c*). Square wave frequency modulation (SWFM) is closely related to both PFM and analogue FM, consisting essentially of a series of square wave edge transitions occurring at the zero crossing points of FM (Fig. 3*d*).

PWM and PPM are both long-established techniques and have been widely adapted for use in optical fibre applications [5–11]. They are far easier to multiplex in the time domain because of their fixed frame timing intervals, and require only a moderately simple demultiplexor at the receiving end. PFM has been used extensively for the optical fibre transmission of video and broadcast quality TV signals [12–17], with SWFM being employed for the fibre transmission of HDTV and other wideband instrumentation signals [18–23]. Comparatively little work, however, has been published on PIM and PIWM applied to wideband fibre transmission [13, 24–27]. Recent work on digital PPM has been aimed primarily at long-haul fibre applications [28, 29]. All PTM methods are, of course, equally amenable to wavelength division multiplexing.

3 Theory

3.1 PTM modulation spectrum

All PTM techniques produce modulation spectra that share a common set of features. In each case, modulation gives rise to a diminishing set of sidetones centred around

the carrier (sampling) frequency and its harmonics, separated in frequency by an amount equal to the signal frequency, as illustrated in Fig. 4. The number and strength of the sidetones (the sidetone profile) is a characteristic unique to each PTM technique. In addition, a baseband component is also present for some PTM methods, along with harmonics, depending upon the form of sampling employed in the modulator.

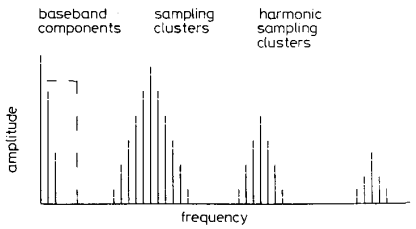

Fig. 4 *Typical PTM modulation spectrum*

Either natural or uniform sampling of the input signal may be adopted for PTM. Naturally sampled modulators operate directly on the input signal, and the precise sampling instants are variable and determined by the location of the modulated pulse edges. For uniform sampling, the input signal is routed via a sample-and-hold circuit which produces flat-topped amplitude-modulated pulses, so that the PTM modulator is operating on uniformly spaced and stored input samples.

Demodulation for natural sampling is effected, after amplitude threshold detection in a PTM receiver, by converting the particular PTM waveform under consideration into a form with a baseband component and filtering out the carrier and sidetone components by a lowpass filter. When uniform sampling is employed, a sample-and-hold circuit is included to recreate an amplitude-modulated pulse form, followed again by a lowpass filter. The choice between natural and uniform sampling is essentially one of performance–cost trade-off, since uniform sampling is, in principle, capable of complete signal recovery without distortion, but with the additional expense of a premium specification sample-and-hold unit.

All PTM techniques display a noise threshold effect below which signal pulses become indistinguishable from noise pulses. Above the threshold, noise occurring during the leading or trailing edges of received PTM pulses manifests itself as timing jitter in the regenerated pulses, and hence as amplitude noise after demodulation. The slope of the received PTM pulse edges determines the period in which noise is able to influence the decoding timing decisions, and therefore the quality of the recovered signal. This mechanism results in demodulated noise power being inversely proportional to the square of the ratio of transmission channel bandwidth to carrier frequency [30], and is responsible for the very useful attribute in PTM of being able to trade off channel bandwidth against signal-to-noise performance.

The approach widely adopted for investigations into PTM modulation spectra is based on a Fourier series expansion of a pulse train modulated by a single sine wave frequency [30–32], rather than assuming a random input signal and employing the autocorrelation of the process to obtain the spectral density of the modulated waveform. In a broad range of transmission applications, such as TV signals, this approach is justified, as the analogue signals will display a dominant subcarrier frequency.

3.2 Classification of pulse time modulation techniques

At present no general method of classifying and categorising PTM modulation techniques has been adopted. However, based on the spectral descriptions outlined in the following sections, an axis of differentiation suitable for the classification of PTM schemes is suggested by considering the behaviour of the sampling waveform's fundamental spectral component under modulation conditions.

For both PWM and PPM this spectral component remains constant in frequency, and never becomes zero under any conditions of modulation, since the internal ramps employed within the modulators are permitted to run their full course without influence from the modulating signal. For this reason, the term 'isochronous' may be adopted when describing PWM and PPM, because of the equal sampling intervals available within their modulation techniques. The duration of the sampling period for both PWM and PPM is determined solely by the choice of carrier (sampling) frequency, and is not affected in any way by the amplitude or frequency of the modulating signal.

However, for the other forms of PTM, the equivalent spectral component is seen either to vanish for certain values of modulation index (PFM and SWFM), or to change in both amplitude and frequency (PIM and PIWM) as a result of the nature of the modulation process. In both cases the effective sampling period utilised within the respective modulators is modified dramatically by the presence of the modulating signal. The classification term 'anisochronous' is therefore most appropriate in these cases, to reflect the unequal sampling periods employed under modulation conditions.

The proposal of a PTM classification system based on the concept of (an)isochronous sampling, as illustrated in Fig. 5, is one which fits naturally with both theoretical and practical considerations. Inspection of spectral predictions from the various modulation formulae will indicate the correct classification category for all existing and any new techniques, and practical spectral measurements will similarly yield an immediate answer by direct observation. Classification in this manner aids modulator testing by predicting suitable calibration features, but has no overt influence on demodulator design, as, in general, a knowledge of carrier frequency behaviour is not required for successful signal recovery.

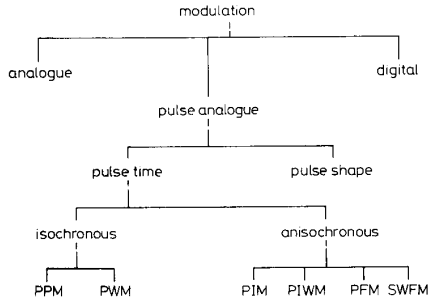

Fig. 5 *PTM classification system*

3.3 Pulsewidth modulation

In pulsewidth modulation (PWM), the width of the pulsed carrier is changed according to the sampled value of the modulating signal, as previously illustrated in Fig. 2*a*. Leading, trailing or double-edge-modulated PWM may be generated by comparison of the input signal with a linear ramp waveform, or triangular in the case of double-edge modulation. For naturally sampled PWM this comparison is performed directly at a comparator, whereas in uniformly sampled PWM the input signal is routed first through a sample-and-hold circuit, so that the input samples are taken at evenly spaced intervals rather than at varying intervals dependent on the signal amplitude, as in Fig. 6*a*. For all styles of PWM (and PPM), a modulation index M $(0 < M < 1)$ may be defined such that maximum modulation occurs when the peak-to-peak amplitude of the input signal is equal to the ramp amplitude, equivalent to a symmetrical peak-to-peak displacement equal to the sampling period for the PWM variable edge or PPM pulse.

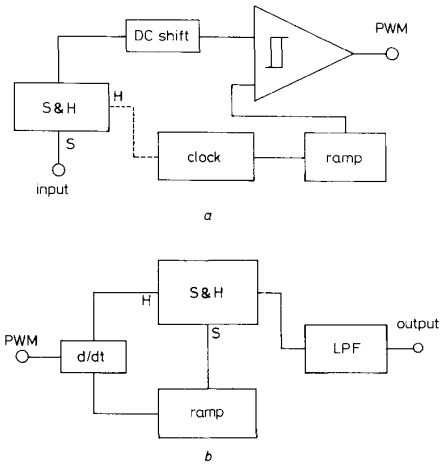

Fig. 6 *PWM modulator and demodulator*
a PWM modulator
b Uniformly sampled PWM demodulator

A comprehensive treatment of the Fourier structure applicable to PWM with a single input tone has been given by Black [30], Bennett [31] and Stuart [32], who have shown that a trailing-edge-modulated naturally sampled PWM waveform with a unity-unmodulated mark/space ratio may be expressed as

$$u(t) = \frac{1}{2} - \frac{M}{2}\sin\omega_m t + \sum_{n=1}^{\infty}\frac{\sin(n\omega_c t)}{n\pi} - \sum_{n=1}^{\infty}\frac{J_0(n\pi M)}{n\pi} \times \sin(n\omega_c t - n\pi) - \sum_{n=1}^{\infty}\sum_{k=\pm 1}^{\pm\infty}\frac{J_k(n\pi M)}{n\pi} \times \sin[(n\omega_c + k\omega_m)t - n\pi] \quad (1)$$

where M is the modulation index $(0 < M < 1)$ and ω_m and ω_c are the modulating signal and carrier frequencies, respectively. $J_k(x)$ is a Bessel function of the first kind, order k.

The second term in eqn. 1 represents the baseband component of ω_m, whereas the combined effect of the third and fourth terms is to produce components at the carrier frequency ω_c and its harmonics. In the unmodulated case $(M = 0)$, only odd harmonics are created, whereas the even harmonics are introduced as M increases. Term 5, involving a double summation, represents the characteristic PTM series of diminishing sidetones set around the carrier frequency and all its harmonics, and separated by a frequency equal to that of the input signal ω_m (Fig. 7*a*). It can be seen from eqn. 1 that the frequency of the sampling (carrier) component is not affected by the value of the modulation index M, and that its magnitude never falls to zero for any level of modulation. For this reason, PWM can be classified as an isochronous PTM technique.

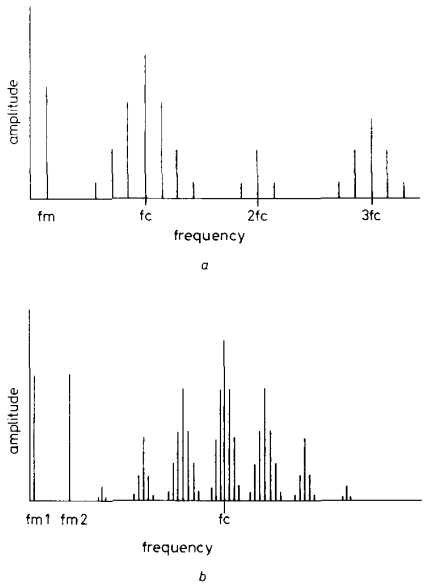

Fig. 7 *PWM modulation spectrum*
a Single-tone naturally sampled PWM
b Double-tone naturally sampled PWM

When uniform sampling is employed in the modulator, the resulting modulation spectrum is very similar [31], except that the baseband now contains in addition a diminishing harmonic series of the modulating signal, influenced not just by the modulation index M, but also by the ratio between the carrier and input signal frequencies.

At the receiver, demodulation in naturally sampled PWM is by threshold detection and a simple lowpass filter to recover the baseband component directly, whereas for uniformly sampled PWM, with its baseband harmonics, conversion into pulse amplitude modulation (PAM) is necessary before lowpass filtering (Fig. 6*b*). The additional complexity of uniformly sampled PWM is offset by the higher maximum modulation index that may be employed, and hence the improved maximum signal-to-noise ratio available.

The basic modulation formula employed to describe and calculate the structure of the PWM spectral modulation components has proved durable by virtue of its

accuracy in predicting the amplitude and frequency of all the sidetone components centred around the sampling frequency and its harmonics. However, it is unable to predict the complex PWM sidetone structure resulting from two or more independent input signals, such as may occur with a complex modulating signal employing subcarriers. As PWM is a nonlinear process the principle of superposition does not apply, and so when two or more independent input signals are considered it is not possible to add their individual Fourier series to give the composite spectrum [33]. Viewing the modulated square wave as a waveform composed of positive and negative staircases, rather than the original double Fourier series adopted by Stuart [32], we have recently derived a spectral prediction formula for two-tone input PWM [34] as

$$\begin{aligned} u(t) = {} & \frac{1}{2} - \frac{M_1}{2}\sin\omega_1 t + \frac{M_2}{2}\sin\omega_2 t + \sum_{n=1}^{\infty}\frac{\sin(n\omega_c t)}{n\pi} \\ & - \sum_{n=1}^{\infty}\frac{J_0(n\pi M_1)J_0(n\pi M_2)}{n\pi}\sin(n\omega_c t - n\pi) \\ & - \sum_{n=1}^{\infty}\sum_{h=\pm 1}^{\pm\infty}\frac{J_0(n\pi M_2)J_h(n\pi M_1)}{n\pi} \\ & \times \sin[(n\omega_c + h\omega_{m_1})t - n\pi] \\ & - \sum_{n=1}^{\infty}\sum_{k=\pm 1}^{\pm\infty}\frac{J_0(n\pi M_1)J_k(n\pi M_2)}{n\pi} \\ & \times \sin[(n\omega_c + k\omega_{m2})t - n\pi] \\ & - \sum_{n=1}^{\infty}\sum_{h=\pm 1}^{\pm\infty}\sum_{k=\pm 1}^{\pm\infty}\frac{J_h(n\pi M_1)J_k(n\pi M_2)}{n\pi} \\ & \times \sin[(n\omega_c + h\omega_{m1} + k\omega_{m2})t - n\pi] \end{aligned} \quad (2)$$

Eqn. 2 represents a naturally sampled PWM waveform employing a square carrier wave of frequency ω_c modulated by two independent frequencies ω_{m1} and ω_{m2}, with modulation indices M_1 and M_2, respectively. The novelty of the equation resides in the triple summation of term 8, whereby a series of diminishing subsidetones of spacing ω_{m2} set around all the ω_{m1} diminishing sidetones is generated. Fig. 7*b* illustrates the character of this subsidetone structure set around all the primary sidetones, along with the sidetones around the carrier fundamental. If either ω_{m1} or ω_{m2} is removed, the spectral structure reverts to the usual single-tone modulation pattern predicted by the original formula, as in either case $J_0(0) = 1$ in the appropriate term 6 or 7, along with $J_{\neq 0}(0) = 0$ for term 8.

An enhanced ability to predict these subsidetone structures will be of importance in PWM applications such as TV and video signals, where strong simultaneous input frequency components are present in the form of colour and sound subcarriers.

When employing PWM, or indeed any of the PTM techniques, for the transmission of TV and video, it is possible to generate low-level 'beats' in the demodulated picture because of interactions between the carrier (sampling) frequency and the colour subcarrier. To avoid this problem it is necessary to adopt an integral ratio between the PTM carrier frequency and the colour subcarrier frequency. A value of 3 : 1 is the lowest practicable ratio because of the nature of PAL and NTSC broadcast TV signal formats and sampling requirements. A higher ratio will result in improved picture quality, since it has a direct influence on reconstructed differential phase error acting via sidetone coincidence [35].

3.4 Pulse position modulation

In PWM, the wasted portion of transmitted power that conveys no information depends on the maximum level of modulation that may be employed. Pulse position modulation (PPM) is the result when the wasted element is subtracted from PWM. This power saving represents the fundamental advantage of PPM over PWM. PPM may be considered as differentiated PWM, and carries information by virtue of the continuously variable position of a narrow pulse within a fixed timeframe (Fig. 2*b*). As the pulsed carrier in this format may be made very narrow, it is well suited for use with injection laser diodes (ILDs). A typical naturally sampled PPM modulator is very similar to a PWM modulator, and consists simply of a comparator detecting equivalence between the input signal and a linear ramp, followed by a monostable or other pulse-generating circuit. Since the main feature of PPM is its power efficiency, no additional pulses are transmitted for frame timing purposes, these being reconstructed within the demodulator.

Employing similar notation as in previous sections, the naturally sampled PPM modulation spectrum may be represented by [32]

$$\begin{aligned} f(t) = {} & \frac{A\omega_c\tau}{2\pi} + AM\cos(\omega_m t)\sin(\omega_m\tau/2) \\ & + \frac{2A}{\pi}\sum_{k=-\infty}^{\infty}\sum_{n=1}^{\infty}J_k(n\pi M)\frac{\sin[(n\omega_c + k\omega_m)\tau/2]}{k} \\ & \times \cos[(n\omega_c + k\omega_m)t] \end{aligned} \quad (3)$$

where τ represents the width of PPM pulses of amplitude A.

Spectral components are generated at the sampling frequency and all its harmonics, along with diminishing groups of sidetones separated by the modulating frequency. Modulation sidetones centred around the sampling frequency and all its harmonics are influenced by both the carrier pulsewidth and the modulating frequency. If the pulse duration is increased, the overall sampling frequency harmonic profile is modified by a sinc (x) function, and eventually becomes similar to that of PWM. This has little effect in practice, as, in general, only low-order carrier harmonics are retained in most transmission applications.

The PPM modulation spectrum also contains a baseband component, composed of a differentiated version of the modulating signal, whose amplitude is dependent on both pulsewidth and input frequency. Demodulation in its simplest form is by integration and lowpass filtering after threshold detection, but more usually consists of converting the PPM pulse stream to PWM, using a bistable and recovered clock pulses, and then lowpass filtering to recover the original signal [36] (Fig. 8*b*). Correct reconstruction of clock pulses is usually arranged by a simple phase-locked loop technique arranged to servo the DC component of the reconstructed analogue signal to zero [37]. If a DC-coupled transmission capability is desired, then frame timing pulses must be included in the PPM pulse stream.

Digital PPM is a relatively new method in which the analogue message is first digitally encoded, as in a PCM system. This digital signal is then further encoded by replacing packets of typically up to 16 bits with a single PPM pulse, whose position allocation within the frame interval is determined uniquely by the code sequence of the associated packet [28, 29] (Fig. 2*c*). Improved detection sensitivity can then be traded against clock rate.

This modulation scheme is aimed primarily at long-haul fibre backbones and deep space communications, where

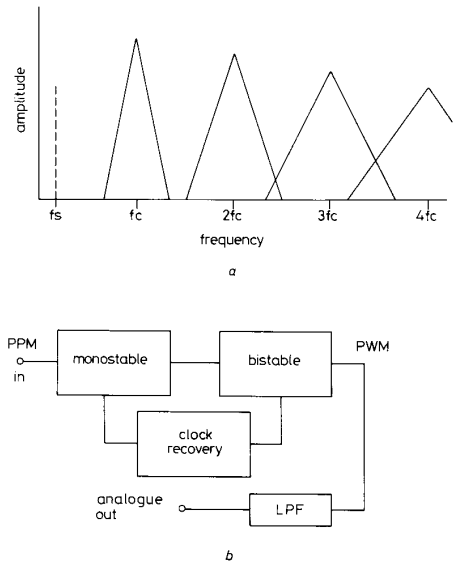

Fig. 8 *Pulse position modulation*
a PPM modulation spectrum
b PPM demodulation

it is desirable to trade transmission bandwidth with repeater spacing, and where the cost of coding complexity can be readily absorbed.

3.5 Pulse interval modulation

As its name suggests, in pulse interval modulation (PIM) the interval between adjacent pulses is determined by the amplitude of the input signal. The format falls into the anisochronous category, as the duration of each sampling episode is determined by the input modulating signal. Fig. 9*a* illustrates one possible implementation of a PIM modulator, where a comparator and ramp generator are connected as a feedback loop to reset the ramp when equivalence is detected between the ramp and the DC-shifted input signal. In the absence of an input signal, the PIM output is a series of uniformly spaced narrow pulses at a free-running frequency determined by both the ramp slope and the unmodulated DC level. The addition of a DC level to the input signal is necessary to ensure that there is always sufficient headroom to accommodate the full dynamic range, and to enable the ramp to sample the most negative input swings. A sample-and-hold unit is inserted in the input lead for uniform sampling, triggered from the comparator output. This is omitted for natural sampling. A modulation index M $(0 < M < 1)$ may be defined in this context as the peak-to-peak modulating signal swing divided by twice the DC level. Operation at very high levels of modulation index should normally be avoided with PIM, as the negative swing of the shifted modulating signal approaches near to zero and hence the instantaneous frequency of the resulting PIM pulse train increases rapidly.

Following the same general approach as Fyath [38], based on earlier derivations [39, 40] but adopting an

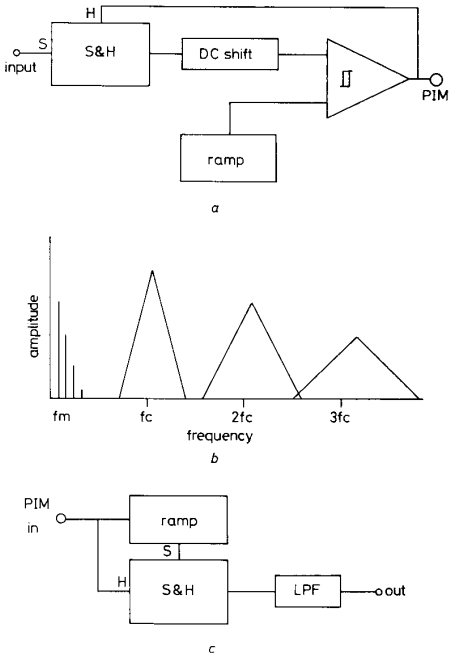

Fig. 9 *Pulse interval modulation*
a PIM modulator
b Modulation spectrum
c PIM demodulator

expansion based on multiple angles, we may present the PIM modulation spectrum as

$$p(t) = \left(\frac{\omega_0}{2\pi}\sum_{p=0}^{\infty} M^p \cos^p \omega_m t\right) \times \left\{1 + 2\sum_{k=\pm 1}^{\infty}\sum_{n_1=-\infty}^{\infty}\sum_{n_2=-\infty}^{\infty} J_{n_1}(kB_1)J_{n_2}(kB_2) \times \cos\left[(kA_0\omega_0 + (n_1 + 2n_2)\omega_m)t\right]\right\} \quad (4)$$

where

$$A_p = \sum_{r=0}^{\infty}(M/2)^{2r}\frac{(p+2r)!}{(p+r)!\,r!} \quad (p = 0, 1, 2)$$

and

$$B_p = \frac{2\omega_0}{p\omega_m}(M/2)^p A_p \quad (p = 1, 2)$$

Here the frequency of the unmodulated unity strength impulse stream is ω_0, with an input signal frequency of ω_m.

The sidetone spectral profiles around the modulated sampling frequency and its harmonics resulting from eqn. 4 are somewhat asymmetrical and a strong function of the modulation index (Fig. 9*b*). There is also a series of baseband harmonics generated in addition to the original

baseband component. In contrast to PPM, the magnitude of the baseband components is not influenced by the input frequency. As the depth of modulation is increased, the average sampling frequency increases from its free-running value.

PIM demodulation is effected for low values of modulation index (typically less than 10%) by simply lowpass filtering to regain the original modulating signal, along with a diminishing series of harmonic distortion components. A more general approach, applicable to the full modulation range, uses the PIM pulses to reset and initiate a ramp whose maximum values constitute sampled points on the reconstructed modulating waveform (Fig. 9*c*). Final filtering takes place either by a low-pass filter or by a combination of sample-and-hold followed by a lowpass filter if uniform sampling has been adopted in the modulator. The noise performance of PIM is marginally superior to PPM under similar conditions [24], but displays a frequency-squared term in its noise power spectral density, which can be problematic in certain applications [41].

3.6 Pulse interval and width modulation

Pulse interval and width modulation (PIWM) is derived directly from its counterpart PIM, by passing PIM pulses through a bistable to produce a waveform in which both mark and space convey information. Both natural and uniform sampling may be employed in a modulator design identical to the PIM case (Fig. 9*a*) except for the addition of a bistable element at the output. As with PIM, the anisochronous nature of PIWM arises because the modulator ramp is reset at a point in time determined by the instantaneous value of the input signal and not by a predetermined interval controlled by the choice of carrier (sampling) frequency.

Employing the same general approach as Fyath [38] for PIM, but adopting an expansion based on multiple angles, we have recently obtained a general PIWM spectral expression given by [27, 42]

$$g(t) = \frac{V}{2}\left\{1 + \sum_{k=1}^{\infty}\sum_{n_1=-\infty}^{\infty}\sum_{n_2=-\infty}^{\infty} \frac{\sin(k\pi/2)}{k\pi/2} J_{n_1}(kB_1) \times J_{n_2}(kB_2)\cos\left[(kA_0\omega_0 + (n_1 + 2n_2)\omega_m)t\right]\right\} \quad (5)$$

where

$$A_p = \sum_{r=0}^{\infty}\left(\frac{M}{2}\right)^{2r}\frac{(p+2r)!}{(p+r)!\,r!} \quad (p = 1, 2)$$

and

$$B_p = \frac{2\omega_0}{p\omega_m}(M/2)^p A_p$$

where M is the modulation index ($0 < M < 1$), V is the amplitude of the PIWM waveform, A_0 is calculated from A_p, and $p = 0$.

Eqn. 5 is a close approximation based on a restricted expansion in which $p = 1, 2$ only, as both B_p and $J_n(kB_p)$ diminish very rapidly for higher values of p.

The PIWM spectral profile resulting from eqn. 5 is asymmetrical and contains no baseband component, in contrast to PIM. Strong spectral components are generated around the modulated sampling frequency $A_0\omega_0$ and all its odd harmonics, surrounded by a diminishing series of sidetones separated by a frequency equal to the modulating frequency ω_m (Fig. 10*a*). The profile of this sidetone structure changes considerably as a function of both M and the ratio ω_0/ω_m. In this respect, the sidetone structure of PIWM more closely resembles square wave FM than PWM.

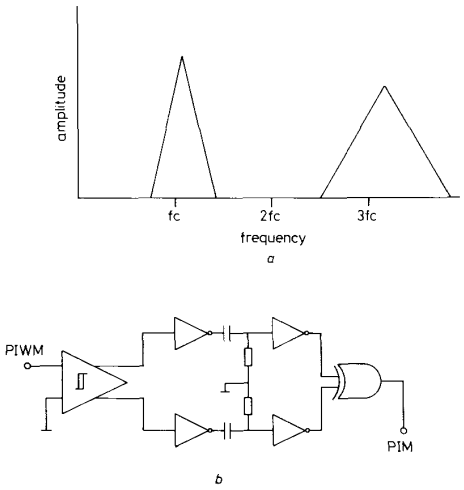

Fig. 10 *PIWM modulation and conversion*
a PIWM modulation spectrum
b PIWM to PIM convertor

For PIM, the minimum permitted ratio of sampling frequency to modulating frequency is 2 : 1, to satisfy sampling theorem requirements. To generate PIWM, the PIM pulses have been divided by two through a bistable, reducing the minimum ratio of ω_0/ω_m to unity for PIWM. This does not violate sampling theory requirements, however, as a PIWM wavetrain carries information on both rising and falling edges, effectively taking two samples per cycle and permitting economic usage of the spectrum. The interval between adjacent sampling instants is therefore identical for both PIM and PIWM.

In contrast to isochronous techniques such as PWM and PPM, the sampling frequency $A_0\omega_0$ is not fixed but increases as the modulation index M increases. For values of M less than approximately 50%, A_0 may be approximated by $1 + M^2/2$. For instance, when $M = 0.2$, $A_0 = 1.02$, shifting the effective sampling frequency upwards by 2%. The magnitude of each sidetone component cannot be calculated by employing a single index m, as is the usual practice, but must be calculated from the combination $n_1 + 2n_2 = m$. Fortunately, the resulting Bessel functions decrease rapidly, making it rarely necessary to use more than three pairs of values for n_1 and n_2 to achieve good accuracy.

Demodulation is carried out by first converting the PIWM waveform to PIM pulses, and then employing PIM demodulation techniques. This process is facilitated by the use of a complementary output stage within the receiver, feeding pairs of logical inverters configured as differentiators followed by an OR gate to recombine the two pulse streams (Fig. 10*b*). At low sampling ratios, PIWM displays up to 4 dB higher signal-to-noise ratio than PPM under identical conditions, whereas this position is reversed at high sampling ratios [43].

3.7 Pulse frequency modulation

In pulse frequency modulation (PFM), the instantaneous frequency of a train of narrow pulses is determined by the modulating signal amplitude. PFM modulation can be conveniently and simply performed by using a voltage-controlled multivibrator (VCM) followed by a circuit to generate low duty cycle pulses (Fig. 11*a*). Below carrier frequencies of approximately 20–30 MHz, standard voltage-controlled multivibrators from the TTL logic family are suitable, whereas above this frequency ECL devices become increasingly necessary.

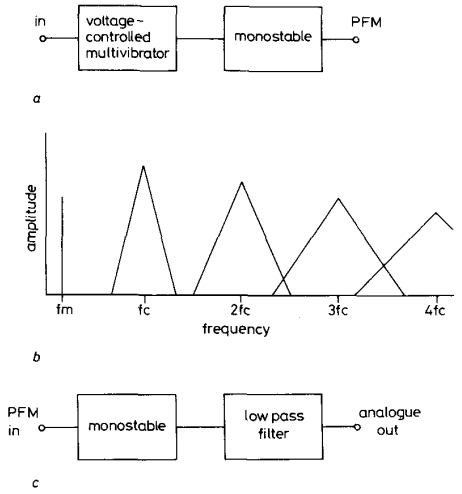

Fig. 11 *Pulse frequency modulation*
a PFM modulator
b PFM modulation spectrum
c PFM demodulator

The PFM spectrum for a series of pulses of width τ and repetition frequency ω_c when modulated by a sine-wave of frequency ω_m to a frequency deviation $\Delta\omega$ may be represented by [2]

$$v(t) = \frac{A\omega_c\tau}{2\pi}\left\{1 + \frac{2M}{\omega_c\tau}\sin(\omega_m\tau/2)\cos(\omega_m t - \omega_m\tau/2) + 2\sum_{n=1}^{\infty}\sum_{k=-\infty}^{\infty} J_k(nM)\frac{\sin(n\omega_c + k\omega_m)\tau/2}{n\omega_c\tau/2} \times \cos[(n\omega_c + k\omega_m)t - k\omega_m\tau/2]\right\} \quad (6)$$

where $M = (\Delta\omega/\omega_m)$ is the modulation index.

As with other frequency modulation techniques, operation with a modulation index greater than unity is possible due to the manner in which the parameter is defined.

Neglecting the DC term, an unmodulated pulse carrier consists of the fundamental and harmonics of the pulse train whose amplitudes follow a $(\sin x)/x$ envelope determined by the pulsewidth τ. Under modulation conditions, the PFM spectrum consists of a baseband component along with a sidetone pattern set around the carrier frequency and all its harmonics (Fig. 11*b*). This sidetone pattern is slightly asymmetrical, with the upper sidetones being stronger than their lower sidetone counterparts. Unlike PWM and PPM, the number of sidetones appearing around any particular carrier harmonic is not determined solely by the amplitude of the input signal, but is also a function of input frequency, as with other FM techniques. As the effective modulation index for any harmonic is proportional to the harmonic number, a large degree of sidetone overlap can occur around harmonics at high values of M. PFM can be classified as an anisochronous PTM technique, as the carrier frequency component in the modulation spectrum will vanish when the modulation index M is equal to 2.405 (as a consequence of $J_0(2.405) = 0$).

Demodulation is usually achieved by threshold detection and some form of monostable to produce equal-length pulses, followed by lowpass filtering to directly recover the baseband signal component from the PFM modulation spectrum [16] (Fig. 11*c*). However, a 3 dB improvement in recovered signal-to-noise ratio can be obtained under most conditions by employing double-edge detection and pulse generation [44, 45], as illustrated in the following section. In common with other PTM techniques, PFM also displays a noise threshold below which the noise performance of the system rapidly deteriorates. For PFM operating above the threshold, the demodulated noise spectrum is not flat but contains an element inversely proportional to the square of the input signal frequency [46, 47], as with other frequency modulation techniques.

3.8 Square wave frequency modulation

Square wave frequency modulation is an anisochronous PTM technique closely related to PFM, and is the pulse equivalent of sine wave frequency modulation (FM), consisting essentially of a series of square wave edge transitions occurring at the zero crossing points of FM, as shown in Fig. 3*d*. The modulation spectrum of SWFM is composed of an FM-like spectrum at the carrier fundamental frequency ω_c with slightly modified forms at all odd harmonics (Fig. 12*a*). The sideband pattern around the nth harmonic of the carrier frequency displays a frequency deviation of n times the deviation around the carrier fundamental. Thus the spectral spreading around each carrier harmonic can be calculated from Carson's rule if desired. The modulation spectrum with an input frequency ω_m may be expressed analytically as [18, 21]

$$s(t) = AD\sum_{n=-\infty}^{\infty}\operatorname{sinc}(n\pi D)\sum_{k=-\infty}^{\infty} J_k(nM) \times \exp[j(n\omega_c + k\omega_m)t] \quad (7)$$

where A is the pulse amplitude, D is the duty cycle, M is the modulation index and J_k is a Bessel function of the first kind, order k.

When the carrier wave is a perfect square wave with a 50% duty cycle ($D = 0.5$) there is no baseband component to the spectrum. However, departure from an accurate 50% duty cycle will result in the generation of a baseband component as well as noticeable FM sidebands at even harmonics of ω_c, along with an increasingly skewed sideband amplitude distribution. Extreme asymmetry in the carrier-wave duty cycle produces a modulation spectrum very similar to that of PFM, where the relative power of the higher-order terms increases with decreasing pulsewidth, indicating that PFM requires a wider transmission bandwidth than SWFM to achieve the same signal-to-noise ratio. By virture of the carrier null experienced when the modulation index M is equal

to 2.405, there exists a well defined point for convenient SWFM system calibration.

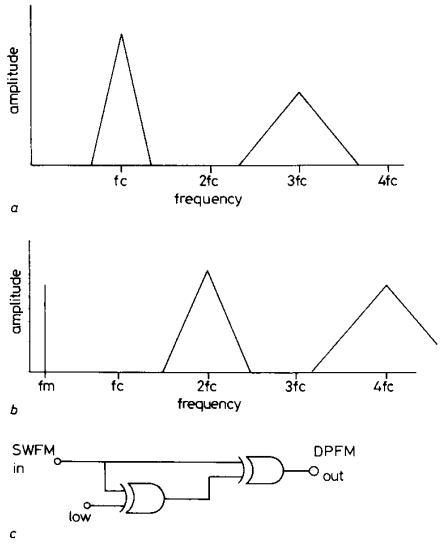

Fig. 12 *Squarewave frequency modulation*
a SWFM modulation spectrum
b Double-edge PFM spectrum
c Double-edge SWFM demodulator

SWFM modulation can be conveniently and easily performed by using a voltage-controlled multivibrator (VCM) with a square wave output, preceded by a lowpass filter to bandlimit the modulating signal.

Methods for demodulation may be deduced directly from the SWFM modulation spectrum. Ordinary FM demodulation techniques may be adopted, locked on to the carrier or harmonics using a phase-locked loop (PLL). However, limited linearity and noise performance usually result from this approach, as a consequence of selecting only a restricted spectral slice. Of more interest is the approach based on pulse regeneration, where either the leading or the trailing edges, or preferably both, of the SWFM waveform are used to reconstruct the associated PFM modulation spectrum, as this contains a baseband component that can then be selected directly by a lowpass filter.

PFM spectral reconstruction from single-edge detection produces a spectrum similar to Fig. 11*b*, in which, along with the desired baseband component, there are sideband structures around every harmonic of the carrier frequency. In contrast, for double-edge detection, only the even harmonics are present above the baseband region (Fig. 12*b*). This produces greater spectral efficiency via a lower bandwidth overhead penalty by lowering the minimum SWFM carrier frequency ω_c necessary for any particular maximum modulating signal frequency ω_m. In addition, there is a doubling of the reconstructed PFM modulation index, resulting in superior signal-to-noise performance compared to the single-edge case [44].

Practical circuit implementation of double-edge baseband pulse regeneration has been found to be particularly simple by employing a number of exclusive OR logic gates in a logic-rectification and delay circuit [18], rather than the usual monostable approach, as in Fig. 12*c*. Again, TTL logic families are adequate for carrier frequencies up to approximately 20–30 MHz, but beyond this value ECL devices must be employed.

4 PTM performance potential

The high-speed performance potential of PTM techniques may be explored by reference to the interactions between spectral occupancy, distortion and signal-to-noise ratio. The suitability of a particular technique for the transmission of analogue data can be evaluated by its ability to produce low distortion concurrent with a low sampling ratio and a high signal-to-noise ratio. From the standpoint of spectral overlap between the modulating signal and the carrier fundamental lower sidetone structure, we can predict the minimum carrier frequency for each of the PTM methods [48].

As all PTM methods operate via time–amplitude conversion, jitter in the transmission system is of concern to the system designer. In general, pulse jitter generated in a PTM modulator and optical transmitter is negligible compared to contributions from other sources [17]. The main jitter contribution is through shot noise and thermal noise in the optical detector and receiver lowering the carrier-to-noise ratio at the demodulator. Above the threshold, where edge noise begins to dominate impulse noise, that is, beyond a carrier-to-noise ratio of around 20 dB [46], PTM pulse slicing and regeneration should occur at half pulse amplitude for minimum jitter penalty through symmetrical eye closure. This may not be the case for an active network that includes fibre amplifiers or optically amplified receivers, where a lower decision threshold may be appropriate due to the asymmetrical eye pattern used to counter the effects of signal-dependent noise through amplifier spontaneous emission [49]. As with most other high-speed fibre systems, transimpedance receiver topologies tend to dominate, due to the higher bandwidths and the absence of equalisation problems, even though there is a small noise penalty from the feedback resistor. The gain of an APD photodetector in a high-sensitivity system must be balanced as usual against its excess noise to minimise the overall noise input to the demodulator.

All the PTM techniques share a very similar spectral modulation structure, with sidetones appearing around the carrier (sampling) frequency and its harmonics, as discussed in a previous section. However, there are particular differences between the techniques concerning the presence of a baseband component and detailed behaviour of the carrier frequency lower sidetone profile which will determine the minimum sampling ratio for a specified distortion behaviour.

PWM and narrowband PPM share an identical sidetone structure around the sampling fundamental, resulting in a ratio of recovered signal modulation level A_m to lower sidetone amplitude A_k of

$$A_m/A_k = \pi M/2J_k(\pi M) \tag{8}$$

where $J_k(\beta)$ is a Bessel function of the first kind, order k and argument β. M is the modulation index.

From this, A_m/A_k can be plotted as a function of M for a range of sampling ratios R, given by f_c/f_m, to gain insight into the limit on distortion imposed by intrusion of the sidetone structure into the recovered baseband. Fig. 13 illustrates that, to obtain a distortion level of 1% (−40 dB), for example, in the recovered signal at its maximum frequency, a minimum sampling ratio R of 4 at

10% modulation index is required, rising to 6 at an index of 70%. (A modulation index of 70–80% is typically the maximum value feasible in PTM modulators before the onset of additional circuit nonlinearities.) These data may be recast as in Fig. 14, to produce design curves indicating the minimum sampling ratio required for specific

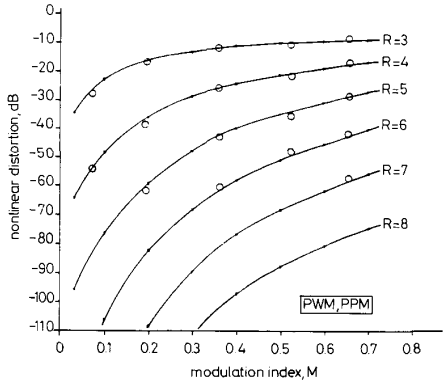

Fig. 13 *Distortion behaviour of PWM and PPM*
theoretical
experimental

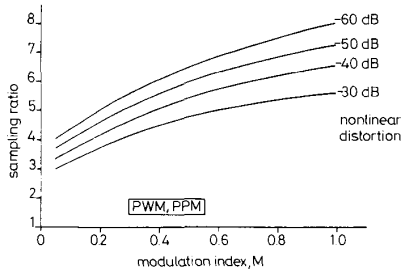

Fig. 14 *Sampling ratios for isochronous PTM*

levels of distortion. Clearly, both PWM and PPM are unlikely to be operated with sampling ratios below 6–7 to obtain low distortion behaviour. Their main attribute is that of circuit simplicity.

For PFM, the ratio of recovered signal component to carrier sidetone level may be expressed as

$$A_m/A_k = \pi\,\Delta f\tau/\sin\,[\pi(f_c + kf_m)\tau]J_k(M) \qquad (9)$$

where Δf is the carrier frequency excursion (also expressible as Mf_m) and τ is the PFM pulse width, with $k = R - 1$.

Fig. 15 illustrates the behaviour of PFM in this respect, showing that, at around a modulation index of 0.5, a minimum sampling ratio of 5 is necessary to obtain a 1% distortion level, increasing to 7 at $M = 2.0$. From the standpoint of bandwidth utilisation for a specified level of nonlinear distortion, PFM modulation is marginally superior to PWM and PPM.

For SWFM with double-edge pulse regeneration demodulation, we may write the ratio of recovered signal-to-sidetone level as [18]

$$A_m/A_k = 2\pi\,\Delta f\tau/\sin\,[\pi(2f_c + kf_m)\tau]J_k(2M) \qquad (10)$$

Eqn. 10 for SWFM differs from the PFM eqn. 9 in that the sidetones are now generated around the carrier second harmonic $2f_c$, with complete suppression of the

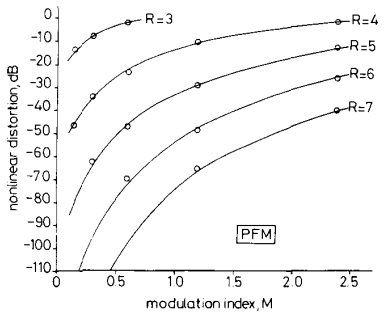

Fig. 15 *Distortion behaviour of PFM*
theoretical
experimental

spectral structure around the carrier fundamental for a unity mark/space ratio carrier wave. In addition, the recovered baseband signal level is twice that of PFM. This results in a superior distortion performance from SWFM for a given sampling ratio, as demonstrated in Fig. 16, producing a minimum sampling ratio of 3 for 1% distortion at $M = 0.5$, rising to 5 at $M = 2.0$.

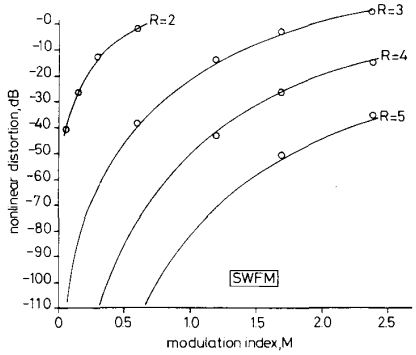

Fig. 16 *Distortion behaviour of SWFM*
theoretical
experimental

A comparison between SWFM and PFM is drawn in Fig. 17, where the minimum required sampling ratio is plotted for a range of distortion performance levels as a function of the modulation index. SWFM is clearly markedly superior to PFM in this respect, achieving theoretical distortion levels due to sidetone incursion of better than −60 dB under modulation conditions where PFM can only achieve −30 dB. In turn, PFM is superior to PWM under similar modulation conditions, making SWFM the best choice from the standpoint of minimum sampling ratio and bandwidth overhead.

In addition to the trade-off between the minimum carrier frequency and distortion performance, we are also interested in the interaction between the signal-to-noise performance and the received pulse edge speed, as dic-

tated by the transmission channel bandwidth B_t. The unweighted improvement factor IF, given by signal-to-noise ratio SNR minus carrier-to-noise ratio CNR,

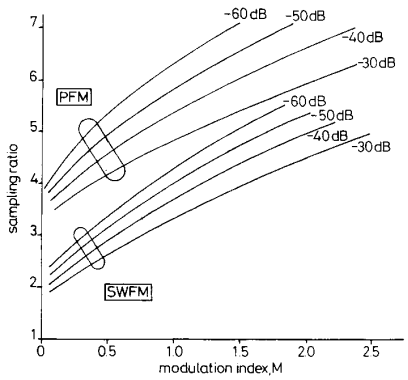

Fig. 17 *Sampling ratios for anisochronous PTM*

expressed in dB, varies above threshold as the square of the ratio of transmission channel bandwidth to carrier frequency. The constant of proportionality is slightly different for each of the PTM techniques [18], such that

$$\text{PWM} \quad IF = \pi^2/8(mB_t/f_c)^2 \tag{11}$$

$$\text{PPM} \quad IF = \pi^2/4(mB_t/f_c)^2 \tag{12}$$

$$\text{PFM} \quad IF = 3/4(mB_t/f_c)^2 \tag{13}$$

$$\text{SWFM} \quad IF = 3/2(mB_t/f_c)^2 \tag{14}$$

To provide an illustrative comparison, Fig. 18 highlights the improvement factor achievable from each of the PTM techniques under the constraint of limiting the transmission channel bandwidth B_t to be 1 GHz, a factor of 10 higher than the maximum signal frequency f_m of 100 MHz in this example, along with a PPM and PFM pulsewidth of 100 ps. This method of presentation is

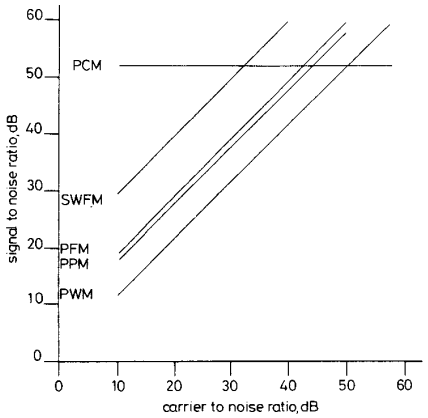

Fig. 18 *Improvement factors for the PTM family*
B_t = 1 GHz
f_s = 100 MHz
τ = 100 ps

informative, as it directly takes into account the different sampling ratio behaviour of each technique. A distortion level of −40 dB is taken as the criterion for choosing the appropriate modulation index and sampling ratio for each technique. The theoretical performance of 8-bit PCM above threshold is also included for comparison, demonstrating that, at high carrier-to-noise ratios, PTM methods become progressively superior.

At a modulation index of 0.5, with the minimum permitted sampling ratio of 5, PWM can only achieve an improvement factor of just under 2 dB. Under the same conditions, PPM is able to achieve 7.8 dB, with PFM returning a marginally better result of 9.5 dB with a modulation index of 1.1 and a sampling ratio of 5.5. Due to the lower sampling ratio required by SWFM for the same level of distortion performance, this technique is able to achieve a superior improvement factor of 20 dB, with a modulation index of 0.9 and a sampling ratio of 3.5, making it the preferred PTM choice when transmission bandwidth is at a premium.

5 Conclusions

This paper has surveyed and reviewed the range of PTM techniques available and outlined their advantages from the standpoint of bandwidth-efficient modulation. A general classification method has been proposed by which different members of the PTM family may be categorised. Equations have been presented to describe the modulation spectrum for each of the methods. The interaction between distortion performance and minimum sampling ratio as a result of sidetone overlap has been examined to explore the high-frequency potential of PTM. Calculations have indicated that, operating above threshold, SWFM could, for example, offer an improvement factor of almost 20 dB for a system restricted to a transmission channel bandwidth of 1 GHz operating with a maximum input signal frequency of 100 MHz.

6 References

1 COOKE, D., JELONEK, Z., OXFORD, A.J., and FITCH, E.: 'Pulse communication', *J. IEE*, 1947, **94**, Part IIIA, pp. 83–105
2 FITCH, E.: 'The spectrum of modulated pulses', *J. IEE*, 1947, **94**, Part IIIA, pp. 556–564
3 JELONEK, Z.: 'Noise problems in pulse communication', *J. IEE*, 1947, **94**, Part IIIA, pp. 533–545
4 LEVY, M.M.: 'Some theoretical and practical considerations of pulse modulation', *J. IEE*, 1947, **94**, Part IIIA, pp. 565–572
5 SCHROCKS, C.B.: 'Proposal for a hub controlled cable television system using optical fiber', *IEEE Trans.*, 1979, **CATV-4**, pp. 70–77
6 BERRY, M.C.: 'Pulse width modulation for optical fibre transmission' (PhD Thesis, Nottingham University, England, 1983)
7 BERRY, M.C., and ARNOLD, J.M.: 'Pulse width modulation for optical fibre transmission of video'. IEE Int. Conf. on the Impact of VLSI Technology on Communication Systems, London, 1983
8 SUH, S.Y.: 'Pulse width modulation for analog fiber-optic communications', *IEEE J.*, 1987, **LT-5**, (1), pp. 102–112
9 WILSON, B., and GHASSEMLOOY, Z.: 'Optical pulse width modulation for electrically isolated analogue transmission', *J. Phys. (E)*, 1985, **18**, pp. 954–958
10 WILSON, B., and GHASSEMLOOY, Z.: 'Optical PWM data link for high quality analogue and video signals', *J. Phys. (E)*, 1987, **20**, (7), pp. 841–845
11 WILSON, B., and GHASSEMLOOY, Z.: 'Optical fibre transmission of multiplexed video signals using PWM', *Int. J. Optoelectron.*, 1989, **4**, pp. 3–17
12 HEATLEY, D.J.T.: 'Video transmission in optical fibre local networks using pulse time modulation'. ECOC 83 — 9th European Conference on Optical Communication, Geneva, September 1983, pp. 343–346
13 OKAZAKI, A.: 'Still picture transmission by pulse interval modulation', *IEEE Trans.*, 1979, **CATV-4**, pp. 17–22

14 HEATLEY, D.J.T.: 'Unrepeatered video transmission using pulse frequency modulation over 100 km of monomode optical fibre', *Electron. Lett.*, 1982, **18,** pp. 369–371
15 HEATLEY, D.J.T., and HODGKINSON, T.G.: 'Video transmission over cabled monomode fibre at 1.5 μm using PFM with 2-PSK heterodyne detection', *Electron. Lett.*, 1984, **20,** pp. 110–112
16 HEKER, S.F., HERSKOWITZ, G.J., GREBEL, H., and WICHANSKY, H.: 'Video transmission in optical fiber communication systems using pulse frequency modulation', *IEEE Trans. Commun.*, 1988, **36,** (2), pp. 191–194
17 KANADA, T., HAKODA, K., and YONEDA, E.: 'SNR fluctuation and non-linear distortion in PFM optical NTSC video transmission systems', *IEEE Trans.*, 1982, **COM-30,** (8), pp. 1868–1875
18 LU, C.: 'Optical transmission of wideband video signals using SWFM' (PhD Thesis, University of Manchester Institute of Science and Technology, Manchester, England, 1990)
19 POPHILLAT, L.: 'Video transmission using a 1.3 μm LED and monomode fiber', 10th European Conf. on Optical Communications, Stuttgart, W. Germany, 1984, pp. 238–239
20 SATO, K., AOYGAI, S., and KITAMI, T.: 'Fiber optic video transmission employing square wave frequency modulation', *IEEE Trans.*, 1985, **COM-33,** (5), pp. 417–423
21 WILSON, B., GHASSEMLOOY, Z., DARWAZEH, I., LU, C., and CHAN, D.: 'Optical squarewave frequency modulation for wideband instrumentation and video signals'. IEE Colloquium on Analogue Optical Communications', London, 1989, Digest 1989/165, Paper 9
22 WILSON, B., GHASSEMLOOY, Z., and LU, C.: 'Optical fibre transmission of high-definition television signals using squarewave frequency modulation'. Third Bangor Symposium on Communications, University of Wales, Bangor, May 1991, pp. 258–262
23 WILSON, B., GHASSEMLOOY, Z., and LU, C.: 'Squarewave FM optical fibre transmission for high-definition television signals' (Fibre Optics 90, 1990, London), *Proc. Int. Soc. Optical Eng.*, 1990, **1314,** pp. 90–97
24 OKAZAKI, A.: 'Pulse interval modulation applicable to narrowband transmission', *IEEE Trans.*, 1978, **CATV-3,** pp. 155–164
25 SATO, M., MURATA, M., and NAMEKAWA, T.: 'Pulse interval and width modulation for video transmission', *IEEE Trans.*, 1978, **CATV-3,** (4), pp. 166–173
26 SATO, M., MURATA, M., and NAMEKAWA, T.: 'A new optical communication system using the pulse interval and width modulated code', *IEEE Trans.*, 1979, **CATV-4,** (1), pp. 1–9
27 WILSON, B., GHASSEMLOOY, Z., and CHEUNG, J.C.S.: 'Spectral predictions for pulse interval and width modulation', *Electron. Lett.*, 1991, **27,** (7), pp. 580–581
28 CALVERT, N.M., SIBLEY, M.J.N., and UNWIN, R.T.: 'Experimental optical fibre digital pulse position modulation system', *Electron. Lett.*, 1988, **24,** (2), pp. 129–131
29 CRYAN, R.A., UNWIN, R.T., GARRATT, I., SIBLEY, M.J.N., and CALVERT, N.M.: 'Optical fibre digital pulse-position-modulation assuming a Gaussian received pulse shape', *IEE Proc. J.*, 1990, **137,** pp. 89–96
30 BLACK, H.S.: 'Modulation theory' (Van Nostrand, New York, 1953), Chapter 17
31 BENNET, W.R.: 'New results in the calculation of modulation components', *Bell Syst. Tech. J.*, 1933, **12,** pp. 228–243
32 STUART, R.D.: 'An introduction to Fourier analysis' (Chapman and Hall, London, 1962), Chapter 6
33 WILSON, B., and GHASSEMLOOY, Z.: 'Multiple sidetone structure in pulse width modulation', *Electron. Lett.*, 1988, **24,** pp. 516–518
34 WILSON, B., GHASSEMLOOY, Z., and LOK, A.: 'Spectral structure of multitone pulse width modulation', *Electron. Lett.*, 1991, **27,** (9), pp. 702–704
35 WILSON, B., and GHASSEMLOOY, Z.: 'Differential phase error in pulse width modulated TV transmission systems', *Electron. Lett.*, 1987, **23,** pp. 1133–1134
36 BIASE, V.D., PASSERI, P., and PIETROIUSTI, R.: 'Pulse analog transmission of TV signal on optical fibre', *Alta Frequenza*, 1987, **LVI-N4,** pp. 195–203
37 HOLDEN, W.S.: 'An optical-frequency pulse-position-modulation experiment', *Bell Syst. Tech. J.*, 1975, **54,** (2), pp. 285–296
38 FYATH, R.S., ABDULLAH, S.A., and GLASS, A.M.: 'Spectrum investigation of pulse interval modulation', *Int. J. Electron.*, 1985, **59,** (5), pp. 597–601
39 TRIPATHI, J.N.: 'Spectrum measurement of pulse-interval modulation', *Int. J. Electron.*, 1980, **49,** pp. 415–419
40 SHARMA, P.D., and TRIPATHI, J.N.: 'Signal to noise ratio studies of PIM and PIM–FM systems', *Int. J. Electron.*, 1970, **28,** (2), pp. 129–141
41 MAROUGI, S.D., and SAYHOOD, K.H.: 'Noise performance of pulse interval modulation systems', *Int. J. Electron.*, 1983, **55,** pp. 603–614
42 WILSON, B., GHASSEMLOOY, Z., and CHEUNG, J.C.S.: 'Optical pulse interval and width modulation for analogue fibre communications', *IEE Proc. J.*, 1992, **139,** (6), pp. 376–382
43 MAROUGI, S.D., and SAYHOOD, K.H.: 'Signal-to-noise performance of the pulse interval and width modulation', *Electron. Lett.*, 1983, **19,** pp. 528–530
44 HEATLEY, D.J.T.: 'SNR comparison between two designs of PFM demodulator used to demodulate PFM or FM', *Electron. Lett.*, 1985, **21,** (5), pp. 214–215
45 NAKAMURA, M., KAITO, K., and OZEKI, T.: 'Modal noise reduced PFM transmission by monopulse to twin-pulse conversion', *Electron. Lett.*, 1985, **21,** (7), pp. 307–308
46 DRUKARVE, A.I.: 'Noise performance and SNR threshold in PFM', *IEEE Trans.*, 1985, **COMM-33,** (7), pp. 708–711
47 WEBB, R.P.: 'Output noise spectrum from demodulator in an optical PFM system', *Electron. Lett.*, 1982, **18,** (14), pp. 634–636
48 WILSON, B., GHASSEMLOOY, Z., and LU, C.: 'High-speed pulse time modulation techniques'. OE/Fibers 92, 1992, Boston, USA, Paper 1787-26
49 LANE, P.M., WATKINS, L.R., and O'REILLY, J.J.: 'Distributed microwave filter realisation providing close to optimum performance for multi-gigabit optical communications', *IEE Proc. J.*, 1992, **139,** pp. 280–287